Hindawi Publishing Corporation
International Journal of Antennas and Propagation
Volume 2015, Article ID 165717, 11 pages
http://dx.doi.org/10.1155/2015/165717

Research Article

Slot Parameter Optimization for Multiband Antenna Performance Improvement Using Intelligent Systems

Erdem Demircioglu,[1] Ahmet Fazil Yagli,[1] Senol Gulgonul,[1] Haydar Ankishan,[2] Emre Oner Tartan,[2] Murat H. Sazli,[3] and Taha Imeci[4]

[1]*Turksat International Satellite Cable TV Operator, Golbasi, 06380 Ankara, Turkey*
[2]*Baskent University, Technical Science MYO, Baglica, 06810 Ankara, Turkey*
[3]*Electrics and Electronics Department, Ankara University, Golbasi, 06380 Ankara, Turkey*
[4]*Electrical and Electronics Engineering Department, Istanbul Commerce University, Kucukyali, 34840 Istanbul, Turkey*

Correspondence should be addressed to Erdem Demircioglu; demirciogluerdem@gmail.com

Received 13 August 2015; Revised 28 October 2015; Accepted 2 November 2015

Academic Editor: Ikmo Park

This paper discusses bandwidth enhancement for multiband microstrip patch antennas (MMPAs) using symmetrical rectangular/square slots etched on the patch and the substrate properties. The slot parameters on MMPA are modeled using soft computing technique of artificial neural networks (ANN). To achieve the best ANN performance, Particle Swarm Optimization (PSO) and Differential Evolution (DE) are applied with ANN's conventional training algorithm in optimization of the modeling performance. In this study, the slot parameters are assumed as slot distance to the radiating patch edge, slot width, and length. Bandwidth enhancement is applied to a formerly designed MMPA fed by a microstrip transmission line attached to the center pin of 50 ohm SMA connecter. The simulated antennas are fabricated and measured. Measurement results are utilized for training the artificial intelligence models. The ANN provides 98% model accuracy for rectangular slots and 97% for square slots; however, ANFIS offer 90% accuracy with lack of resonance frequency tracking.

1. Introduction

Microstrip patch antennas (MPAs) have rapidly developing applications in personal communication systems (PCS), direct broadband television (DBT), mobile satellite communication (MSC), wireless local area networks (WLAN), and body area networks (BAN). Low cost and profile with ease of integration to other planar structures, portability, and robustness for implementation on rigid surfaces are well-known advantages of the MPAs [1–4]. Moreover, the MPAs suffer from low gain and efficiency with high loss and narrow bandwidth. Novel antenna designs made effort to overcome these drawbacks by applying various techniques for bandwidth enhancement and multiband radiation.

Single layer multiband antennas can be achieved using reactive loading with stubs [5], monolithic reactive loading [6], adding strips on the patch [7], patch trimming with a rectangular notch [8], or shorting pins [9] for closely spaced bands with frequency ratios around 1.5 : 1. Multiband printed antennas having frequency band separation of 2 : 1 or 4 : 1 employ window concept whereby windows are cut in low frequency patch radiators to accommodate high frequency patch antennas [10–12]. The other way of realizing multiband antennas needs multilayering with two or more metallic patches between one or more dielectric layers. Dichroic and stacking techniques are commonly used methods with disadvantages of fabrication complexity and coupling between stacked patches.

Antenna bandwidth is specified as frequency range over which VSWR is less than 2. This offers a return loss of −9.5 dB or 11% reflected power. Typically antenna bandwidth is assumed to be the frequency region providing return loss lower than −10 dB. Bandwidth enhancement for MPAs can be obtained by increasing patch-ground plane separation using

thicker substrate [3]. Thick substrate causes surface wave modes with increasing mutual coupling, degradations in impedance mismatch, radiation loss, polarization distortion, and scan blindness in phased array antennas [13–15]. MPA bandwidth can also be improved by modifying patch shape by slots, adding resonant structures such as more layers, patches, and extra components and applying various feeding techniques such as microstrip line and coaxial, aperture coupled and proximity coupled feeds.

Soft computing based artificial intelligence techniques have broad application areas on microwave design and production challenges. Bioinspired nature of these techniques allows the microwave equipment designers to avoid repetitive cost of electromagnetic (EM) simulations, manufacturing and test procedures. Artificial neural network (ANN) techniques are well-proven methods for microwave design field including antennas [16], arrays [17], MOSFETs [18], passive components [19], and power amplifiers [20].

Particle Swarm Optimization (PSO) is a population based stochastic optimization technique developed by Kennedy and Eberhart in 1995 [21]. It is a global optimization algorithm, which can effectively be used to solve multidimensional optimization problems by attempting to simulate the swarming behavior of birds, bees, and so forth. PSO can easily be implemented and its performance is comparable to other stochastic optimization technique, such as genetic algorithm and simulated annealing [22, 23]. PSO integrated with analytical methods or full wave simulation techniques have been widely used to design antennas and arrays [24–30].

Differential Evolution (DE) optimization algorithm is a stochastic vector-based population approach [31]. DE is considered as the fastest optimization method on a general basis over Particle Swarm Optimization and the evolutionary algorithm [32]. Since then, it has found wide applications in engineering designs in various fields [33–37].

In this paper, a slotted MMPA design is proposed. The reference geometry [16] has multiband radiation with limited bandwidth capabilities for the interested frequencies. The multiband property is introduced using inverted L shaped stubs to the main patch. Bandwidth enhancement technique of introducing slots is applied to our previous work where nonslotted antenna geometry provides multiband characteristics at 2.83 GHz, 5.76 GHz, 6.57 GHz, and 11.23 GHz. Slotted antennas obtain broad impedance bandwidth along with stability of the radiation patterns. Variation of the slot shape helps in generating additional resonances, which, when coupled to the original resonances of the slot, further increases impedance bandwidths. The antenna gain, radiation pattern, and reflection coefficient are considered as the antenna design constraints. As the symmetrical slots are inserted to the main patch, considerable bandwidth enhancement is explored. However, a generic approach to determine slot parameters is needed. The slot dimensions and distance to the radiating edge are modeled using ANN. Then the ANN architecture is optimized utilizing PSO and DE methods.

In the next section revealing description is given about soft computing based bioinspired modeling techniques and application to proposed problem. In section three, modeling results are compared with each other and the original nonslotted multiband antenna. Optimization results to determine suitable model architectures are also presented in this chapter. The final section briefly concludes the findings with improvements of the proposed methods.

2. Bioinspired Artificial Intelligence Modeling

2.1. Artificial Neural Networks. ANNs are nonlinear soft computing structures with robust generalization ability from collected data. ANNs have the estimation ability for any input value between its training ranges. This shows its generalization and memorizing capability. The generalization ability makes them applicable to RF microwave modeling field with commonly used multilayer perceptron neural networks (MLPNNs) structure and back-propagation algorithm.

MLPNNs include the input, hidden and output layers with synapses to link layers. Each layer has the processing units called neurons to make computations. MLP has been applied successfully to solve diverse problems using supervised training methods with a highly popular algorithm known as the error back-propagation algorithm. Figure 1 represents the proposed MLP network architecture established for the multiresonance antenna slot parameters determination problem.

The physical parameters of antenna slot (slot length/width and slot distance to radiating edge) are utilized as the ANN model input with substrate features and frequency. The return loss of the slotted antenna is modeled and optimum configuration of the slot parameters is determined. Figure 2 represents the 2D layout of the proposed antenna geometry with physical dimensions in both sides.

A simple quarter wave matching line is attached to the antenna feed line at 5 GHz center frequency of the main patch. Since the feed line alternates only the antenna gain and is utilized to match antenna impedance to the SMA connector, its dimensions are not included in the ANN model. Besides the substrate properties slot parameters' ranges for ANN input parameters vary from $6.57\,\text{mm} \leq \text{SL} \leq 18.25\,\text{mm}$, $0.75\,\text{mm} \leq \text{SW} \leq 2.875\,\text{mm}$, and $1.25\,\text{mm} \leq \text{SD} \leq 3.75\,\text{mm}$. Both the matching line and the peeled substrate area around proposed antenna are added to the board in order to simplify manufacturing and obtain accurate measurement results.

2.2. Adaptive Network Fuzzy Inference System. ANFIS uses a hybrid learning algorithm to identify parameters of Sugeno-type fuzzy inference systems. It applies a combination of least-squares and back-propagation gradient descent methods for training fuzzy inference system membership function's parameters to emulate a given training data set. ANFIS was introduced by Jang in 1993 [38] and it is constructed as a set of fuzzy if-then rules with appropriate membership functions. It specifically has a neurofuzzy type of learning ability with a network having nodes in the five different layers to complete specific functions as shown in the ANFIS architecture in Figure 3.

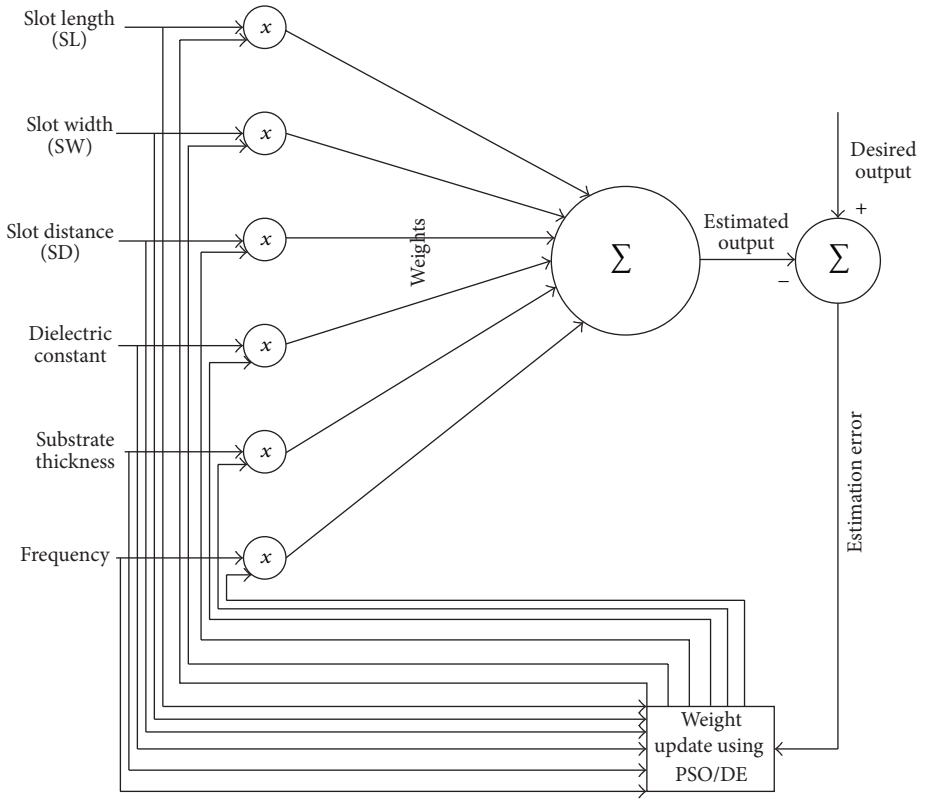

Figure 1: MLPNN architecture for the proposed problem.

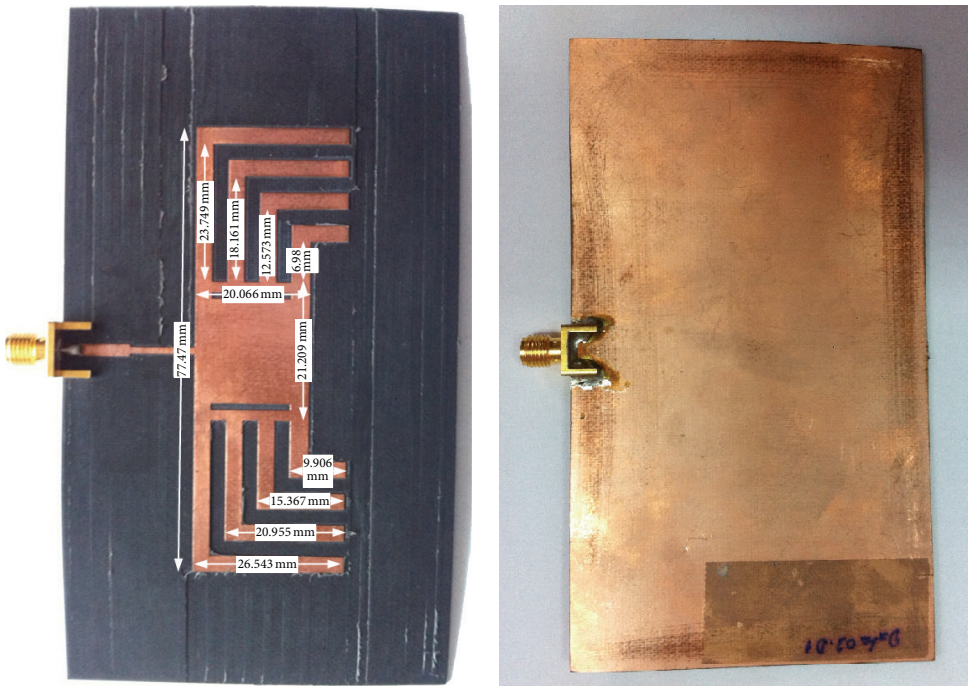

(a) (b)

Figure 2: (a) Fabricated antenna with geometrical dimensions (b) bottom of the antenna.

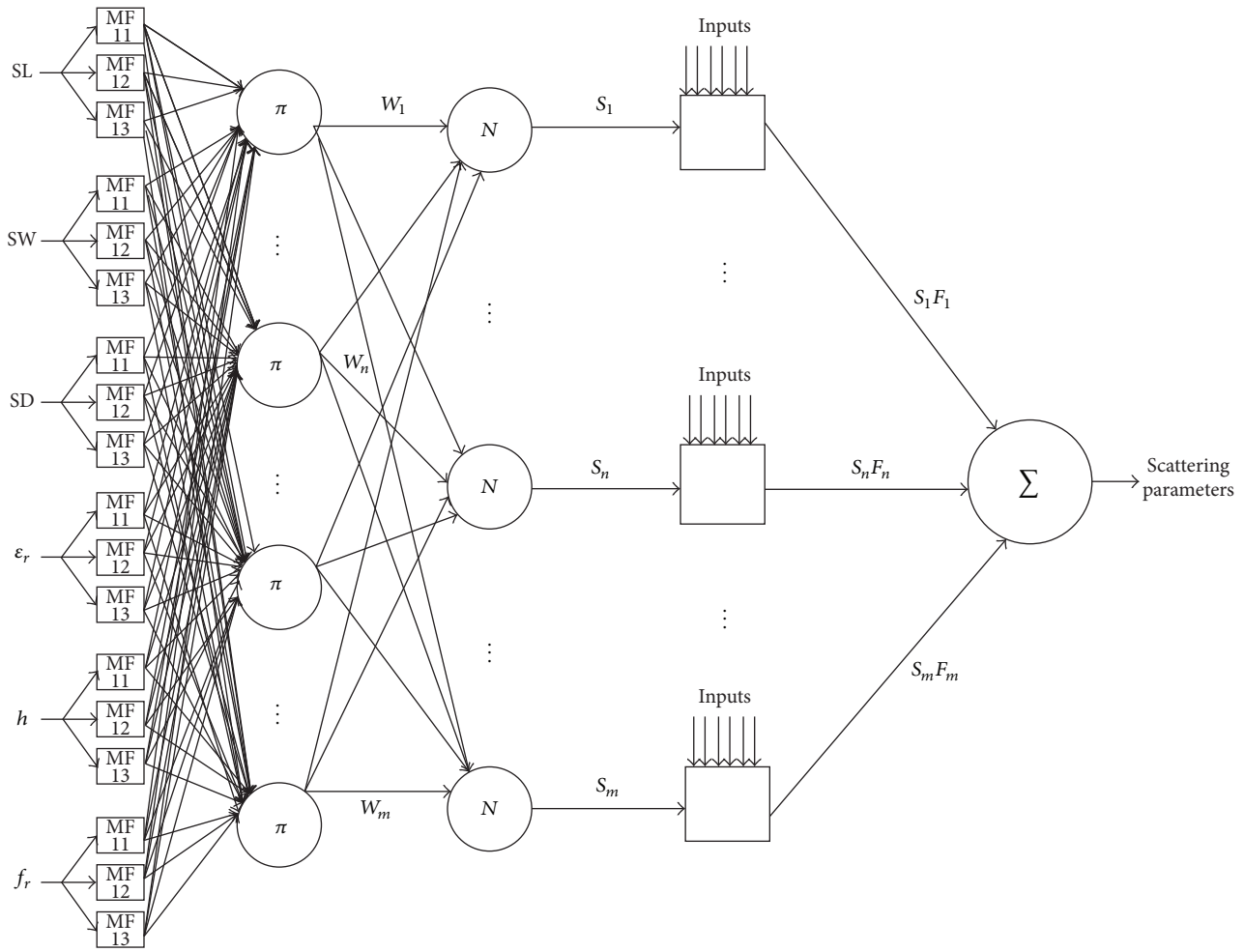

Figure 3: Sugeno-type adaptive neurofuzzy system.

Two fuzzy if-then rules based on a first-order Sugeno model with inputs x and y are equated as follows.

Rule 1

$$\text{if } (x \text{ is } A_1) \text{ and } (y \text{ is } B_1)$$
$$\text{then } (f_1 = p_1 x + q_1 y + r_1). \tag{1}$$

Rule 2

$$\text{if } (x \text{ is } A_2) \text{ and } (y \text{ is } B_2)$$
$$\text{then } (f_2 = p_2 x + q_2 y + r_2). \tag{2}$$

A_i and B_i are fuzzy sets, f_i is outputs within the fuzzy region specified by the rules, and p_i, q_i, and r_i are the design parameters that are determined during the training process.

The black box model of the proposed antenna is given in Figure 4 for MLPNN and ANFIS approximates. Initially input(s) and output(s) parameters of the black box are defined; then data sets are generated with full ranges of input parameters using measurements and simulations. Once the measurement data is applied for ANN/ANFIS modeling, trained model should estimate accurate results and iteration of test and measurement steps can be reduced which lead to the manufacturing cost at a minimum level.

3. Optimization of Modeling Architecture

A multilayer feedforward perceptron ANN consists of interconnected neurons over consecutive layers. The neuron output is scaled by a weight and fed forward as an input through a nonlinear activation function to the succeeding layer neurons. This structure leads to a trained ANN performing nonlinear mapping between input and output vectors. The training process is based on updating the weights according to the error between input and output data in every epoch. Despite the common use of the back-propagation (BP) algorithm for the training, its vital drawback is the local optima problem. This may be encountered due to the gradient based method. Since the BP depends on gradient based method, the random initialization of weights may lead to missing global optima and getting stuck in local optima. As the dimension order is high and the problem is complex, search space can contain many local optimum points. Conversely metaheuristic algorithms avoid this problem by

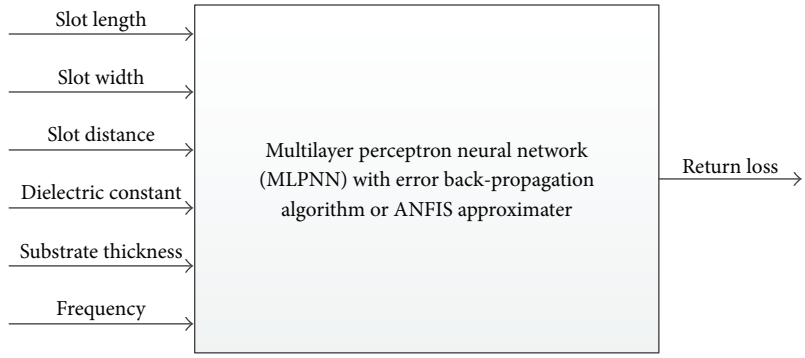

Figure 4: Black box representation of ANN/ANFIS approximates.

providing diversity for potential solutions in search space. Therefore, instead of BP, regarding global search capabilities, evolutionary computation algorithms are applied for ANN training. In this study, local optima problem is tested using two evolutionary computation algorithms, Particle Swarm Optimization (PSO) and Differential Evolution (DE).

3.1. Differential Evolution (DE). Differential Evolution (DE) is an evolutionary optimization algorithm introduced by Storn and Pricer [31]. DE has been applied in many real world problems as well as benchmark functions. DE has a simple yet efficient algorithm which makes it suitable for global optimization problems. Basically the algorithm is based on diversifying the population according to the scaled vector differences and updating next generation using greedy scheme.

The algorithm can be given in four steps.

Initialization. In DE, the population that contains potential solutions is named target population represented by X. ith member of X is a target vector x_i. N_p target vectors are initialized in search space randomly as follows:

$$x_{j,i} = b_{j,l} + \text{rand}_j \cdot \left(b_{j,u} - b_{j,l}\right), \tag{3}$$

where $b_{j,u}$ is the upper bound and $b_{j,l}$ is lower bound of search space, respectively. $j = 1, 2, \ldots, D$ represents the dimension number of the vector x_i and rand_j is random number between 0 and 1.

Mutation. DE applies two operators for population diversity. Firstly, mutation operator is applied to obtain a mutant vector v_i to be used in the later crossover stage. There are several DE variants represented as DE/x/y/z. In this representation x denotes the base vector, y denotes the number of difference vectors used, and z represents the crossover method. In classic variant of DE, represented as DE/rand/1/bin, mutant vector is obtained as

$$v_i = x_{r_0} + F \cdot \left(x_{r_1} - x_{r_2}\right). \tag{4}$$

In classic variant of DE, represented as DE/rand/1/bin, mutant vector is obtained as

$$v_{i,g} = x_{r_0,g} + F \cdot \left(x_{r_1,g} - x_{r_2,g}\right), \tag{5}$$

where r_0, r_1, and r_2 are randomly chosen distinct indexes and different from target index i. the scale factor, $F \in (0, 1+)$, is a positive number generally selected smaller than 1. In this study for the purpose of fast convergence we adopt DE/best/1/bin version which uses the best vector as the base vector. Then the mutant vector is given as

$$v_{i,g} = x_{\text{best},g} + F \cdot \left(x_{r_1,g} - x_{r_2,g}\right). \tag{6}$$

Crossover. In crossover, the mutant vector and the target vector are recombined to produce a trial vector u_i that is a candidate for new target vector. The parameters at jth dimension of two vectors are mixed, according to a random number rand_j between 0 and 1. If rand_j is smaller or equal to the predetermined crossover probability C_r, parameter of trial vector takes the jth parameter from mutant vector; otherwise, target vector's parameter is taken. To ensure that there is at least one parameter different from target vector, the dimension that is equal to a random index number rand_j is changed as mutant:

$$u_{i,j} = \begin{cases} v_j; & \text{if } \left(\text{rand}_j \le C_r \text{ or } j = j_{\text{rand}}\right) \\ x_j; & \text{otherwise,} \end{cases} \tag{7}$$

where u_i is the trial vector.

Selection. Selection is carried out by a simple greedy scheme that compares the objective function values of target and trial vectors. The vector that has a better objective function value takes place in the next generation as target vector.

By repeating this loop for every target vector, a generation is completed and the population is updated.

3.2. Particle Swarm Optimization (PSO). The Particle Swarm Optimization (PSO) is an evolutionary computation algorithm inspired by social behavior of bird flocking and fish schooling. As a population based algorithm like other evolutionary algorithms, PSO updates its members using a predefined fitness function. In the search process PSO mimics the inspired swarm behavior according to fitness function to update the population. In PSO each member named particle x_i keeps track of the overall best position and its best position

Table 1: Fabricated rectangular slotted antenna properties.

Prototype name	Slot length	Slot width	Slot distance
Prototype A	730	30	100
Prototype B	545	85	100
Prototype C	545	115	100
Prototype D	545	40	75

in hyperspace. Each particle tends to its best position p_i and the population's best position g_i achieved thus far. These are called local best and global best, respectively. In the position update a velocity term v_i is added to the particle's present position x_i. The velocity includes the particle's previous scaled velocity and the movements towards local and global best positions. The velocity and position updates are given as follows:

$$v_i = w * v_i + c_1 * \text{rand}_1 * \left(p_g - x_i\right) + c_2 * \text{rand}_2 * \left(p_i - x_i\right), \quad (8)$$

$$x_i = x_i + v_i. \quad (9)$$

In (8) c_1 and c_2 are acceleration constants that determine the rate of movements towards local best and global best. Rand_1 and rand_2 are random numbers between 0 and 1, which are used to diversify movement directions. w is the inertia weight that helps to improve convergence by scaling previous velocity. Here the adopted variable weight, w, is initialized as 0.9 and decreased to 0.4 at the end of maximum generations.

4. Modeling and Optimization Results

The proposed antennas are designed with various Rogers Duroid substrates using method of moments based AWR AXIEM solver. Selected samples (RT/duroid 5880 with ε_r = 2.2 and substrate thickness of 0.775 mm) are fabricated using LPFK milling machine and measured with Agilent E5071C ENA series network analyzer. The bandwidth enhancement can be achieved by increasing substrate thickness or introducing slots into the main patch. The slot parameters, distance to radiating edges, width, and length are manipulated to attain the optimum antenna geometry.

Frequency, dielectric constant, and substrate thickness are also taken as the input parameters since they directly affect antenna characteristics. In this study, the substrate thickness varies from 0.775 mm to 3.125 mm, the dielectric constant, ε_r, is taken as 2.2 or 2.94, and the measurement frequency range alters from 1 GHz to 15 GHz.

4.1. Modeling Results. Symmetrical rectangular dual slots are applied with altering distances to radiating patches between 1.25 and 3.75 mm. Slot lengths and widths are varied from 6.75 to 18.25 mm and 0.75 to 2.875 mm, respectively. Above all simulations, 4 slotted prototypes are fabricated to gather measurement data. The fabricated prototype antenna parameters are given in Table 1.

Simulated and measured results for slotted antennas are illustrated with nonslotted multiband antenna to compare

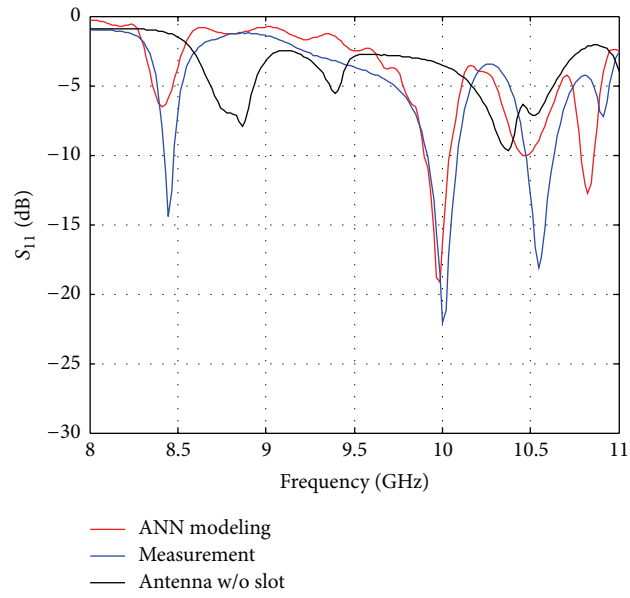

Figure 5: Bandwidth and resonance enhancement for 8 GHz to 11 GHz range of Prototype B.

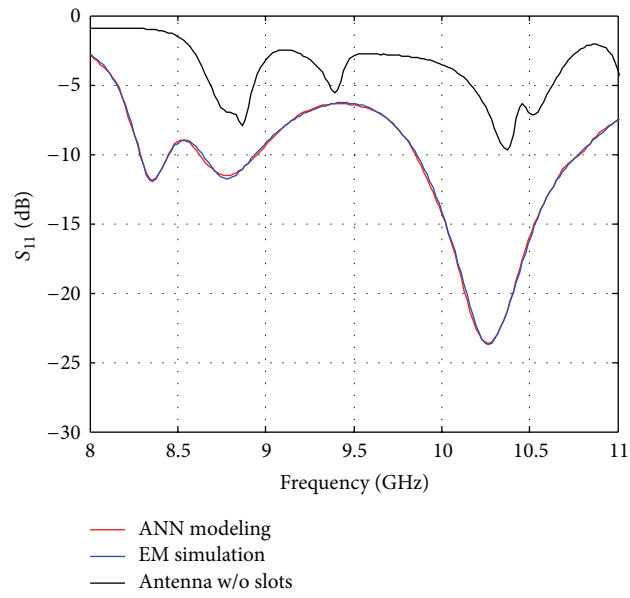

Figure 6: Bandwidth enhancement for 8 GHz to 11 GHz range by thickening substrate.

the bandwidth enhancement and resonance characteristics. The optimum slot parameters (length, width, and distance values) and substrate selection are determined using artificial intelligence techniques. In Figure 5, the frequency band of 8 GHz to 11 GHz of Prototype B is given. The bandwidth and resonance enhancements can be observed compared to nonslotted antenna among frequency range with slight center frequency shifts.

In Figures 6 and 7, slot and substrate thickness impacts on 8 GHz–11 GHz and 12 GHz–15 GHz frequency ranges are illustrated, respectively. Thickening the antenna substrate is

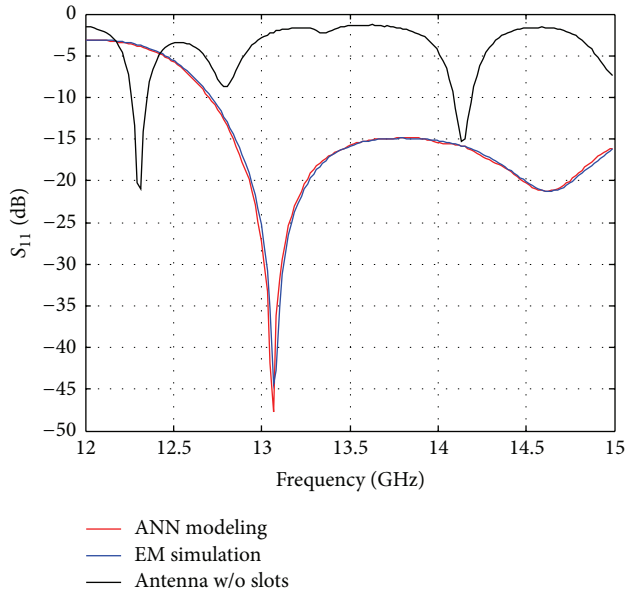

Figure 7: Bandwidth enhancement for 12 GHz to 15 GHz range by thickening substrate.

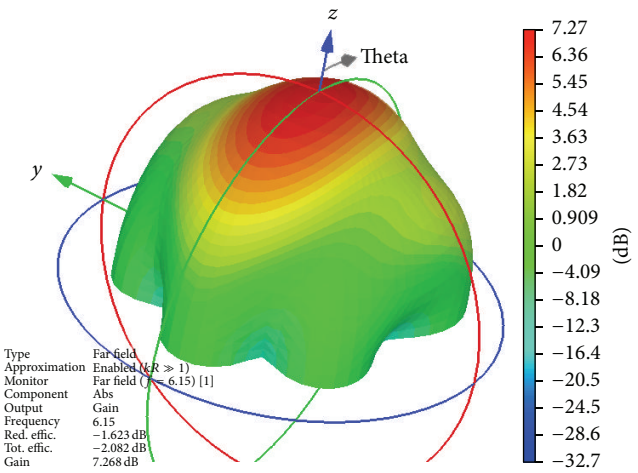

Figure 8: Radiation pattern of Prototype B at 6.15 GHz.

a very well-known technique to improve antenna resonance bandwidth. Besides introducing slots, substrate properties are investigated to improve overall antenna performance. A 3.125 mm thick substrate is applied in order to investigate antenna performance using AWR AXIEM simulator. As seen in Figure 6, center frequency shifts for 8–11 GHz range are considerably limited; however, resonance values improved significantly over a wide range of frequency.

The resonance bandwidth characteristic is improved sufficiently for the frequency band over 13.06 GHz as shown in Figure 7.

The antenna patterns are also examined in order to detect effective radiation characteristics in resonance frequency points. Figure 8 depicts the radiation pattern of Prototype B achieving satisfactory antenna gain for multiband application.

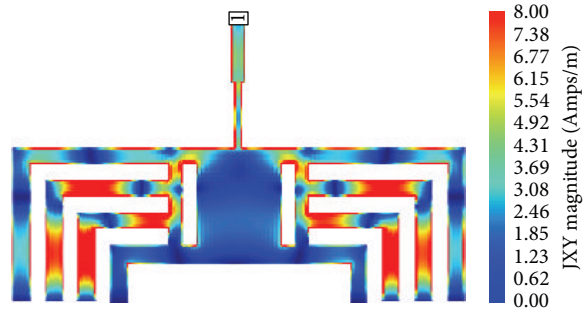

Figure 9: Radiation pattern of Prototype B at 6.15 GHz.

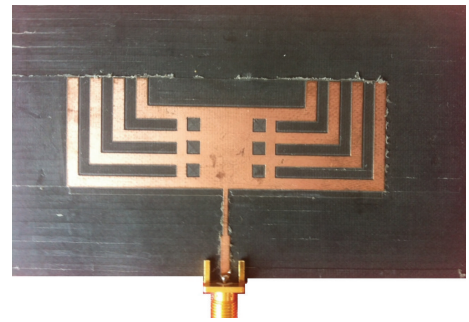

Figure 10: Multiband antenna with 6 symmetrical square slots.

Other than gain, currents on the antenna surface are analyzed for each prototype. Figure 9 illustrates the surface current of the proposed antenna at 6.15 GHz. Antenna has single radiation point with the main patch. As the inverted L stubs are introduced multiband characterization is observed. Prototype B radiates from the second and third stubs at 6.15 GHz since other stubs and main patch have low surface current.

In addition to rectangular slots, square slots are introduced to achieve bandwidth enhancement. Figure 10 shows the manufactured antenna with 6 square slots of 3 mm slot edge dimensions. Slot distance to radiating patch is fixed by 2.5 mm.

In Figure 11 ANN and ANFIS modeling results are compared with slotted antenna measurements. Bandwidth enhancement is achieved at higher frequencies around 10 GHz by introducing square slots compared to original nonslotted antenna. An optimum square slot dimension is determined as 3 mm. It is observed from the antenna spectrum that radiation points diminish and bandwidths shrink while the square slot dimensions are getting larger.

In Table 2, nonslotted antenna and the slotted antenna with thick substrate are compared with antenna performance parameters of bandwidth, resonance frequency, and gain.

4.2. Optimization Results. In this paper, two population based evolutionary optimization algorithms were used to optimize the ANN parameters of the proposed system. Here, DE and PSO parameters were firstly tuned and the experimental results have been compared with derivative

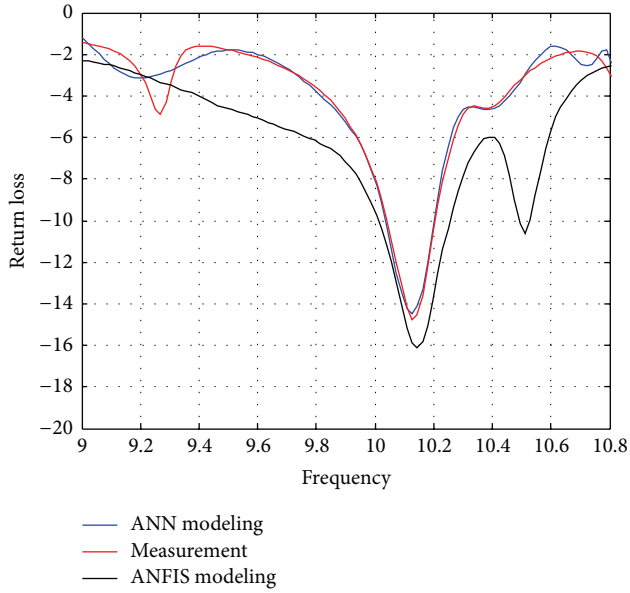

Figure 11: Modeling performance comparison of RT/d 5880 multiband antenna with 3 × 3 mm symmetrical square slots.

Table 2: Comparison of performance parameters for nonslotted and slotted antennas.

Nonslotted antenna		Slotted antenna	
Center frequency (GHz)	4.15	Center frequency (GHz)	4.657
Bandwidth (MHz)	20	Bandwidth (MHz)	260
Gain (dB)	6.91	Gain (dB)	6
Center frequency (GHz)	5.85	Center frequency (GHz)	5.77
Bandwidth (MHz)	50	Bandwidth (MHz)	230
Gain (dB)	8.97	Gain (dB)	8.994
Center frequency (GHz)	11.3	Center frequency (GHz)	10.3
Bandwidth (MHz)	90	Bandwidth (MHz)	925
Gain (dB)	11.44	Gain (dB)	7.76
Center frequency (GHz)	14.95	Center frequency (GHz)	14.6
Bandwidth (MHz)	110	Bandwidth (MHz)	800
Gain (dB)	10.95	Gain (dB)	8.51

based ANN training algorithm. Figure 12 represents the comparison of EM circuit design including traditional method, DE/PSO based design method, and proposed optimization method.

For PSO, three variants have been applied and the best variant's result is given with DE and Back-Propagation Method's results in Table 3.

ANN Training. In this application, an ANN model with two hidden layers is considered. Model with k inputs and z outputs, consisting of m_1 and m_2 neurons, in the first and second hidden layers, respectively, has $k \cdot m_1 + m_1 \cdot m_2 + m_2 \cdot z$ weights and $m_1 + m_2 + z$ thresholds. Therefore, total number of parameters of network will be $D = k \cdot m_1 + m_1 \cdot m_2 + m_2 \cdot z + m_1 + m_2 + z$ and search space in optimization problem will have D dimensions.

Table 3: Comparison of performance results for applied artificial intelligence methods.

	ANN	DE	CPSO	ANFIS
Average	8.136	11.535	11.1353	11.09
Best	7.3243	10.3840	9.9730	9.9328

Mean square error can be used as fitness function to evaluate a member's fitness in the algorithms. The hidden transfer function is sigmoid function and the output transfer is a linear activation function; then the fitness function of the ith member of population is derived as follows:

$$
\begin{aligned}
f\left(s_j\right) &= \frac{1}{\left(1 + \exp\left(-\left(\sum_{i=1}^{n} w_{ij} \cdot x_i - \theta_j\right)\right)\right)}, \\
y_k &= \sum_{j=1}^{T} w_{kj} \cdot f\left(s_j\right) - \theta_k, \\
E &= \sum_{k=1}^{q} \frac{E_k}{(q * M)}, \\
E_k &= \sum_{i=0}^{M} \left(\text{error}_i^k\right), \\
\text{fitness}\left(X_i\right) &= E\left(X_i\right),
\end{aligned}
\tag{10}
$$

where n is the number of input nodes, w_{ij} is the weight from ith node of input layer to jth node of the hidden layer, θ_j is the threshold of the jth hidden layer, x_i is the ith input, s_j is the weight input sum in hidden layer, y_k is the output of kth layer, q is the number of training samples, E is the training error, $j = 1, 2, \ldots, T$, and $k = 1, 2, \ldots, M$.

Differential Evolution (DE) Training. As explained above, DE needs two parameters in population diversity operators. These are scale factor F and crossover probability C_r. These parameters can be tuned according to the optimization problem. Firstly we investigate the suitable F, C_r pair and then use the best pair in the final training procedure. Since both parameters are in the same interval, they can be tested by increment of 0.1 from 0.1 to 1. Incrementing F by 0.1 from 0.1 to 1, meanwhile fixing the C_r and repeating this cycle after each increment of C_r by 0.1 will yield 100 pairs. The performances of networks trained according to these pairs are given in Figure 10 where a set of pairs yield close test errors. Among these pairs the best performance is obtained by $F = 0.4$ and $C_r = 0.9$. Using these values network is trained for 10 times. The average performance of network is obtained as 11.535 where the best performance was 11.0341. Figure 13 depicts the scale factor versus crossover probability of DE.

Particle Swarm Optimization Training. Each PSOPC is run for 10 times, $G_{\max} = 1000$, and an average performance value is recorded. First, a standard PSO with inertia weight is applied and acceleration constants are set as 2. Then a decaying inertia weight ω is adopted as proposed in [39]. ω is initialized to 0.9

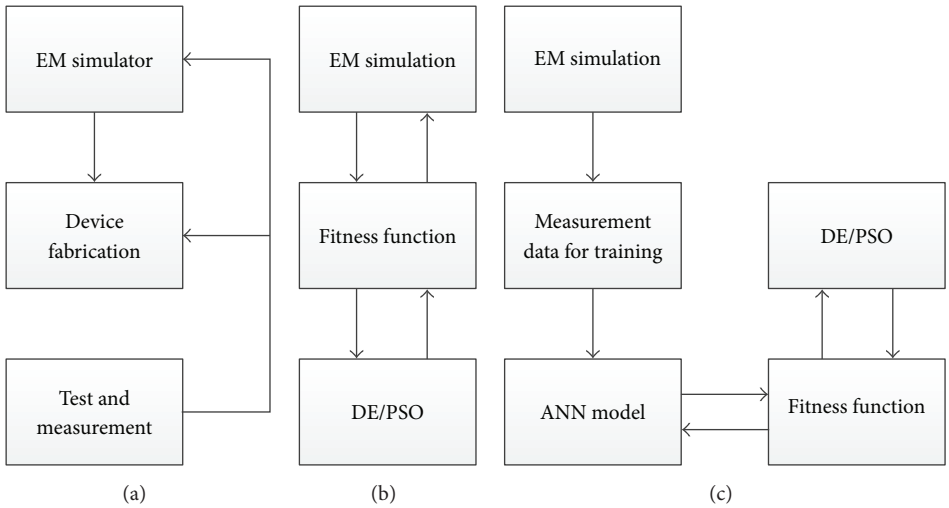

Figure 12: (a) Traditional design method using expert domain knowledge and hit/trial method. (b) Design using DE/PSO by directly appealing EM simulator as its fitness function. (c) Design using proposed method of ANN optimization with DE/PSO.

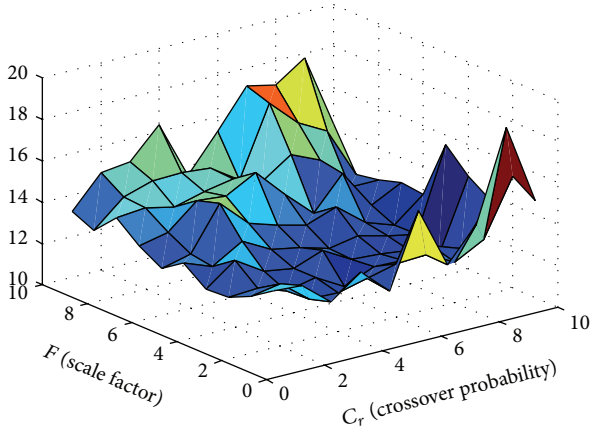

Figure 13: Scale factor versus crossover probability of DE.

and reduced to 0.4 at the final stage. Average performance value is obtained as 13.7989.

Secondly, the acceleration constants are set as 0.5, and passive congregation coefficient is set as 0.6 [40]. Inertia weight is initialized as 0.9 and decreased to 0.7 at the end. The average performance is 11.3670. Finally, CPSO is applied for the calculation of constriction factor using Clerc's method. Acceleration constants c_1 and c_2 are set as 2.05, φ is set to 4.1, and constriction factor is given as $\chi = 0.729$ by [41]. The average performance value was 11.1353. It is observed that among three variants the best average performance is obtained by CPSO. Therefore, best result obtained by CPSO is used for the training of ANN and comparison with other methods.

For the training of the ANN three different methods have been applied in order to obtain the best performance and check local optimality problem. The average and best error values of the ANNs are given in Table 2. As seen from the table among these algorithms, the best result is obtained by the conventional back-propagation algorithm. Therefore, the methods with the best performance have been used to train ANN that has been used to determine optimum antenna shape.

5. Conclusion

Multiband microstrip patch antennas have wide application areas in mobile technology such as GSM, UMTS, LTE, and Bluetooth. However, it is complicated for antenna designers to attain multiband antenna characteristics with enhanced communication bandwidth. Multiband characteristic of the antenna disappears as bandwidth enhancement is applied. In this study, rectangular and square slots are introduced into MMPAs to overcome bandwidth problem. Return loss is determined as the antenna performance parameter and set to the modeling output. Slot dimensions and distance to antenna edge are varied to find optimum slot configuration providing multiple bands and enhanced bandwidth.

The comparisons for variations of slot parameters indicate that, as the slot width increases, antenna return loss lessens and reflections are reduced noticeably. Slot width variations cause slight center frequency oscillations without bandwidth enhancement. Also slot distance to radiating edges is inspected. It is shown that closer slots to radiating patch edge introduce more resonance at lower frequencies. The mean slot distance results are more beneficial in terms of bandwidth enhancement and resonance points compared to far and near ones. Moreover, slot length alternations with fixed slot width and distance are examined. Multiple radiation points and higher bandwidth performances are achieved with an average slot length. Increasing slot length causes disappearance of radiation at lowest frequencies.

The proposed modeling techniques utilize bioinspired artificial intelligence methods to determine optimum antenna shape. Artificial modeling techniques prevent iterative simulation, manufacturing, and test procedures for

microwave equipment. This leads significant support to lower production cost. As the model library improves, equipment development can be implemented using bioinspired techniques.

Conflict of Interests

The authors declare that there is no conflict of interests regarding the publication of this paper.

References

[1] W. L. Stutzman and G. A. Thiele, *Antenna Theory and Design*, John Wiley & Sons, New York, NY, USA, 1998.

[2] C. A. Balanis, *Antenna Theory*, John Wiley & Sons, New York, NY, USA, 2nd edition, 1997.

[3] J. R. James and P. S. Hall, *Handbook of Microstrip Antennas*, Peter Peregrines, London, UK, 1989.

[4] D. M. Pozar and D. H. Schaubert, *Microstrip Antennas: The Analysis and Design of Microstrip Antennas and Arrays*, IEEE Press, New York, NY, USA, 1995.

[5] W. F. Richards, S. E. Davidson, and S. A. Long, "Dual band reactively loaded microstrip antenna," *IEEE Transactions on Antennas and Propagation*, vol. 33, no. 5, pp. 556–561, 1985.

[6] S. E. Davidson, S. A. Long, and W. F. Richards, "Dual band microstrip antennas with monolithic reactive loading," *Electronics Letters*, vol. 21, no. 20, pp. 936–937, 1985.

[7] J. Mcilvenna and N. Kernweis, "Modified circular microstrip antenna elements," *Electronics Letters*, vol. 15, no. 7, pp. 207–208, 1979.

[8] H. Nakano and K. Vichien, "Dual-frequency square patch antenna with rectangular notch," *Electronics Letters*, vol. 25, no. 16, pp. 1067–1068, 1989.

[9] S. S. Zhong and Y. T. Lo, "Single element rectangular microstrip antenna for dual-frequency operation," *Electronics Letters*, vol. 19, no. 8, pp. 298–300, 1983.

[10] M. Negev and C. S. Samson, "Integrating multi-channel and multi-frequency microstrip antenna array," *Microwave and RF Engineer*, vol. 1989, pp. 41–44, 1989.

[11] A. A. Abdelaziz, A. Henderson, and J. R. James, "Dual band circularly polarized microstrip array element," in *Proceedings of the Journées Internationales de Nice sur les Antennes (JINA '90)*, pp. 321–324, Nice, France, November 1990.

[12] A. A. Abdelaziz, "Bandwidth enhancement of microstrip antenna," *Progress in Electromagnetics Research*, vol. 63, pp. 311–317, 2006.

[13] A. K. Bhattacharyya and L. Shafai, "Surface wave coupling between circular patch antennas," *Electronics Letters*, vol. 22, no. 22, pp. 1198–1200, 1986.

[14] L. W. Lechtreck, "Effects of coupling accumulation in antenna arrays," *IEEE Transactions on Antennas and Propagation*, vol. 16, no. 1, pp. 31–37, 1968.

[15] D. M. Pozar and D. H. Schaubert, "Scan blindness in infinite phased arrays of printed dipoles," *IEEE Transactions on Antennas and Propagation*, vol. 32, no. 6, pp. 602–610, 1984.

[16] E. Demircioglu, M. H. Sazli, S. T. Imeci, and O. Sengul, "Soft computing techniques on multiresonant antenna synthesis and analysis," *Microwave and Optical Technology Letters*, vol. 55, no. 11, pp. 2643–2648, 2013.

[17] O. P. Acharya, A. Patnaik, and S. N. Sinha, "Limits of compensation in a failed antenna array," *International Journal of RF and Microwave Computer-Aided Engineering*, vol. 24, no. 6, pp. 635–645, 2014.

[18] Y. Ko, P. Roblin, A. Zarate-de Landa et al., "Artificial neural network model of SOS-MOSFETs based on dynamic large-signal measurements," *IEEE Transactions on Microwave Theory and Techniques*, vol. 62, no. 3, pp. 491–501, 2014.

[19] E. Demircioglu and M. H. Sazli, "Behavioral modeling of a C-Band ring hybrid coupler using artificial neural networks," *Radioengineering*, vol. 19, no. 4, pp. 645–652, 2010.

[20] S. Yan, C. Zhang, and Q.-J. Zhang, "Recurrent neural network technique for behavioral modeling of power amplifier with memory effects," *International Journal of RF and Microwave Computer-Aided Engineering*, vol. 25, no. 4, pp. 289–298, 2015.

[21] J. Kennedy and R. Eberhart, "Particle swarm optimization," in *Proceedings of the IEEE International Conference on Neural Networks*, pp. 1942–1948, Perth, Australia, December 1995.

[22] J. Kennedy and J. M. Spears, "Matching algorithms to problems: an experimental test of the particle swarm and some genetic algorithms on the multimodal problem generator," in *Proceedings of the IEEE World Congress on Computational Intelligence and IEEE International Conference on Evolutionary Computation*, pp. 78–83, Anchorage, Alaska, USA, May 1998.

[23] J. Robinson and Y. Rahmat-Samii, "Particle swarm optimization in electromagnetics," *IEEE Transactions on Antennas and Propagation*, vol. 52, no. 2, pp. 397–407, 2004.

[24] A. Dastranj, H. Abiri, and A. Mallahzadeh, "Two-dimensional synthesis and optimization of a broadband shaped beam reflector antenna using IWO and PSO algorithms," *International Journal of RF and Microwave Computer-Aided Engineering*, vol. 25, pp. 129–140., 2014.

[25] N. Jin and Y. Rahmat-Samii, "Parallel particle swarm optimization and finite-difference time-domain (PSO/FDTD) algorithm for multiband and wide-band patch antenna designs," *IEEE Transactions on Antennas and Propagation*, vol. 53, no. 11, pp. 3459–3468, 2005.

[26] H. Wu, J. Geng, R. Jin et al., "An improved comprehensive learning particle swarm optimization and its application to the semiautomatic design of antennas," *IEEE Transactions on Antennas and Propagation*, vol. 57, no. 10, pp. 3018–3028, 2009.

[27] R. Bhattacharya, T. K. Bhattacharyya, and R. Garg, "Position mutated hierarchical particle swarm optimization and its application in synthesis of unequally spaced antenna arrays," *IEEE Transactions on Antennas and Propagation*, vol. 60, no. 7, pp. 3174–3181, 2012.

[28] L. Lizzi, F. Viani, R. Azaro, and A. Massa, "A PSO-driven spline-based shaping approach for ultrawideband (UWB) antenna synthesis," *IEEE Transactions on Antennas and Propagation*, vol. 56, no. 8, pp. 2613–2621, 2008.

[29] D. Cao, A. Modiri, G. Sureka, and K. Kiasaleh, "DSP implementation of the particle swarm and genetic algorithms for real-time design of thinned array antennas," *IEEE Antennas and Wireless Propagation Letters*, vol. 11, pp. 1170–1173, 2012.

[30] P. Rocca, M. Benedetti, M. Donelli, D. Franceschini, and A. Massa, "Evolutionary optimization as applied to inverse problems," *Inverse Problems*, vol. 25, pp. 1–41, 2009.

[31] R. Storn and K. Price, "Differential evolution—a simple and efficient heuristic for global optimization over continuous spaces," *Journal of Global Optimization*, vol. 11, no. 4, pp. 341–359, 1997.

[32] J. Vesterstrøm and R. Thomsen, "A comparative study of differential evolution, particle swarm optimization, and evolutionary algorithms on numerical benchmark problems," in *Proceedings of the Congress on Evolutionary Computation (CEC '04)*, pp. 1980–1987, June 2004.

[33] S. Das, D. Mandal, R. Kar, and S. P. Ghoshal, "A new hybridized backscattering search optimization algorithm with differential evolution for sidelobe suppression of uniformly excited concentric circular antenna arrays," *International Journal of RF and Microwave Computer-Aided Engineering*, vol. 25, no. 3, pp. 262–268, 2015.

[34] S. Yang, Y. B. Gan, and A. Qing, "Antenna-array pattern nulling using a differential evolution algorithm," *International Journal of RF and Microwave Computer-Aided Engineering*, vol. 14, no. 1, pp. 57–63, 2004.

[35] A. Deb, J. S. Roy, and B. Gupta, "Performance comparison of differential evolution, particle swarm optimization and genetic algorithm in the design of circularly polarized microstrip antennas," *IEEE Transactions on Antennas and Propagation*, vol. 62, no. 8, pp. 3920–3928, 2014.

[36] S. K. Goudos, "Design of microwave broadband absorbers using self-adaptive differential evolution algorithm," *International Journal of RF and Microwave Computer-Aided Engineering*, vol. 19, no. 3, pp. 364–372, 2009.

[37] P. Rocca, G. Oliveri, and A. Massa, "Differential evolution as applied to electromagnetics," *IEEE Antennas and Propagation Magazine*, vol. 53, no. 1, pp. 38–49, 2011.

[38] J.-S. R. Jang, "ANFIS: adaptive-network-based fuzzy inference system," *IEEE Transactions on Systems, Man and Cybernetics*, vol. 23, no. 3, pp. 665–685, 1993.

[39] Y. Shi and R. C. Eberhart, "Modified particle swarm optimizer," in *Proceedings of the IEEE International Conference on Evolutionary Computation (ICEC '98)*, pp. 69–73, Anchorage, Alaska, USA, May 1998.

[40] S. He, J. Wen, E. Prempain, Q. Wu, J. Fitch, and S. Mann, "An improved particle swarm optimization for optimal power flow," in *Proceedings of the International Conference on Power System Technology*, pp. 1633–1637, Singapore, November 2004.

[41] M. Clerc, "The swarm and the queen: towards a deterministic and adaptive particle swarm optimization," in *Proceedings of the Congress on Evolutionary Computation (CEC '99)*, pp. 1951–1957, Washington, DC, USA, July 1999.